LIGO Laboratory / LIGO Scientific Collaboration

LIGO-T040044-01-K

Advanced LIGO UK

March 2004

Interferometric OSEM Sensor Development

Clive Speake, Stuart Aston

(The University of Birmingham)

Distribution of this document:
Inform aligo_sus

This is an internal working note
of the Advanced LIGO Project, prepared by members of the UK team.

Institute for Gravitational Research
University of Glasgow

School of Physics and Astronomy
University of Birmingham
Phone +44 (0) 121 414 6447
Fax +44 (0) 121 414 3722
E-mail av@star.sr.bham.ac.uk

Engineering Department
CCLRC Rutherford Appleton Laboratory

Particle Physics and Astronomy Research Council (PPARC)

http://www.ligo.caltech.edu/

http://www.sr.bham.ac.uk/~sma/aluk_bham.html

http://www.eng-external.rl.ac.uk/advligo/papers_public/ALUK_Homepage.htm

1 Abstract

We describe an interferometer that has been designed as a sensor for control of the pendulum suspensions in Advanced LIGO. The device is a homodyne polarisation-based interferometer that uses a laser diode source. We discuss how the requirements of Advanced LIGO can be possibly met by the current design.

2 Introduction

There has been considerable progress in the field of metrology in the development of accurate and robust interferometric sensors. Of particular interest are the so-called homodyne interferometers[1] which use two or more interferometer outputs to accurately determine displacements with a resolution of much less than one fringe without the need for ac modulation of optical paths. These devices are being used in atomic force microscopes,[2] for example, where absolute displacement accuracy is of importance.

Downs and Raine[1] originally proposed a polarisation based system that used 3 interferometric outputs. Each output, I_n, varies sinusoidally with the target mirror displacement but with phase offsets of zero, $\pi/2$ and π:

$$I_n = I_{out}\left(1 + V\cos\left(\phi + (n-1)\frac{\pi}{2}\right)\right) \tag{1}$$

Where V is the visibility of the fringes, $V = (I_{max} - I_{min})/(I_{max} + I_{min})$, $\phi = \frac{2\pi}{\lambda}\Delta l$, Δl is the optical path length difference and λ is the wavelength of the light used. It is easily shown that ϕ can be determined as:

$$\phi = \arctan\left(\frac{I_1 - I_2}{I_2 - I_3}\right) - \frac{\pi}{4} \tag{2}$$

With,

$$z = \frac{\phi}{2\pi} \cdot \frac{\lambda}{2} \tag{3}$$

This last result follows for a standard Michelson interferometer where the mirror motion is given as $\Delta z \approx \frac{\Delta l}{2}$. Raine and Downs[3,4] further developed a system with only two outputs that was polarisation independent. The phase shift between the outputs was generated by a purpose-

built metallised beam-splitter, although various designs had been employed in metrology laboratories such as the International Bureau of Weights and Measures (BIPM) in France. This system has the advantage that it requires fewer optical components and has an output that is independent of the polarisation state of the source.

In the ideal case described by equation (2) the two difference outputs, when plotted against each other (on an oscilloscope in *x*-*y* mode, for example), describe a circular Lissajous figure centred at the origin. In the case where only two outputs are available the centre of the Lissajous pattern lies at the radius of the pattern, when V is unity, in both *x* and *y* directions. Displacement of $\lambda/2$ of the target mirror in a standard Michelson configuration produces a complete revolution of the Lissajous figure. In order to track the displacement over completed revolutions software must perform equation (2) with at least two measurements per revolution, and sum the number of integer rotations. For the standard Michelson configuration, a sampling frequency of f_s gives a maximum mirror speed of:

$$\dot{z}_{max} = \frac{\lambda}{4} f_s \qquad (4)$$

In practice, imperfections in the optical set-up produce an elliptical Lissajous figure whose centre is displaced from the origin. In the twin output case the effects of changes in the visibility of the fringes cannot be compensated for, for each determination of ϕ. In this case ellipticity and variable visibility can only be accounted for by fitting to a substantial fraction of a complete cycle around the pattern. This sophisticated analysis, rather than equation (2), is also necessary for accurate fringe interpolation. The accuracy of homodyne interferometers can only be guaranteed when used in conjunction with good quality laser sources such as frequency stabilised Helium-Neon lasers. The spacing between longitudinal modes, $\Delta\nu$, is typically GHz for such lasers which leads to a minimum in fringe visibility in the standard Michelson configuration at $z = c/4\Delta\nu$ and to periodicities in the visibility of the fringes for $\Delta z = c/2\Delta\nu$, (typically 10's of cm's).

3 Application to advanced LIGO

For application as an optical sensor for local control (OSEM) in Advanced LIGO the accuracy is of no real importance. Here the emphasis is on the sensitivity and the displacement range. Whilst, clearly it is desirable to achieve as high a sensitivity as possible, the most demanding sensitivity is 1.4×10^{-12} m/rt(Hz). The displacement range is defined as 2.8mm with a maximum velocity of 1mms^{-1}. Other design considerations are heat dissipation due to thermal isolation within the UHV environment, reliability, vacuum compatibility of components, low electromagnetic interference and low wire count and stiffness to avoid shunting active vibration isolation stages. See accompanying document[5] for further details of requirements.

We believe that a homodyne interferometer could provide a suitable device for an OSEM and satisfy these requirements. There have been notable other designs for interferometric sensors for this application such as that due to Gray *et al*[6]. However the combination of sensitivity and displacement range seems to have been elusive.

A first obvious consequence of these design criteria is that He-Ne lasers would not be appropriate due their size. If the sources were located remotely (perhaps outside the vacuum chamber) and fibre couplers employed, there would still be the possible problem of vacuum compatibility of inexpensive fibre cables. Clearly it would be desirable to have a local reliable compact source for each OSEM and the obvious choice is a laser diode. The modal spacing of the output of laser diodes is typically of order 200GHz (see reference [7], for example). This leads to periodicities in the intensities of the interference fringes corresponding to optical path differences of about 0.75mm in a standard Michelson configuration. When operated above threshold the visibility of the fringes remains good despite this variation and the laser diode line-width is of the order MHz for powers of around a mW or so. The threshold temperature for diode lasers is temperature dependent. In order to make the system as robust as possible against variations in fringe visibility it is clearly desirable to use a scheme with at least 3 orthogonal outputs. This strategy appears to exclude the method based on a metallised beam-splitter. In addition the polarisation-based systems can be configured to work at a range of wavelengths, giving the possibility that the most reliable source can be selected. In principle the metallised beam-splitter can be manufactured with coatings appropriate for any wavelength, however the beam-splitters currently available from NPL are optimised to work at 633nm.

It is important that tilts of the suspension do not lead to angular displacement of the measurement beam and loss of interference. The usual way of avoiding this is to use a cat's eye reflector attached to the target whose position is to be measured. The cat's eye can be in the form of a lens / mirror combination or a cube-corner reflector. Clearly we would prefer not to attach the cat's eye to the suspension as this may involve a lossy mount and add a significant moment of inertia. Also the optical axes of the interferometer and cat's eye would then need to be aligned. One possible way forward is to employ a lens at the output of the interferometer and a plain mirror mounted (or preferably in some cases deposited) on the suspension mass. However, in such a system the visibility of the fringe pattern is reduced as the target mirror moves away from the focal plane of the lens. Using the Rayleigh criterion[8] we can estimate the depth of focus for a ray, a distance y from the optical axis:

$$\Delta z \approx \frac{f^2}{y^2}\frac{\lambda}{2} \qquad (5)$$

For $y \approx 1$mm this amounts to 0.5mm even for a 100mm focal length lens. In practice the fringe visibility reduced by approximately 50% for 0.5mm of displacement for a configuration where the beam diameter was about 2mm.

It is clear that an alternative method is required to satisfy the Advanced LIGO requirements. In metrological applications a hybrid retro-reflector is used[9]. This system doubles the potential sensitivity of the laser as the target beam undergoes a double-pass through the retro-reflector. Although this is possibly an advantage, it introduces an asymmetry between the target and reference beam, requiring the length of the reference arm to be doubled. We have developed a novel polarisation-based design which has been adapted from Greco *et al*[10] and which we believe satisfies the Advanced LIGO requirements.

4 Proposed Interferometer

Figure 1 shows a schematic of the device as it could be developed for Advanced LIGO. The diagram is to scale and shows the length and diameter of the cylindrical volume available for the OSEM.

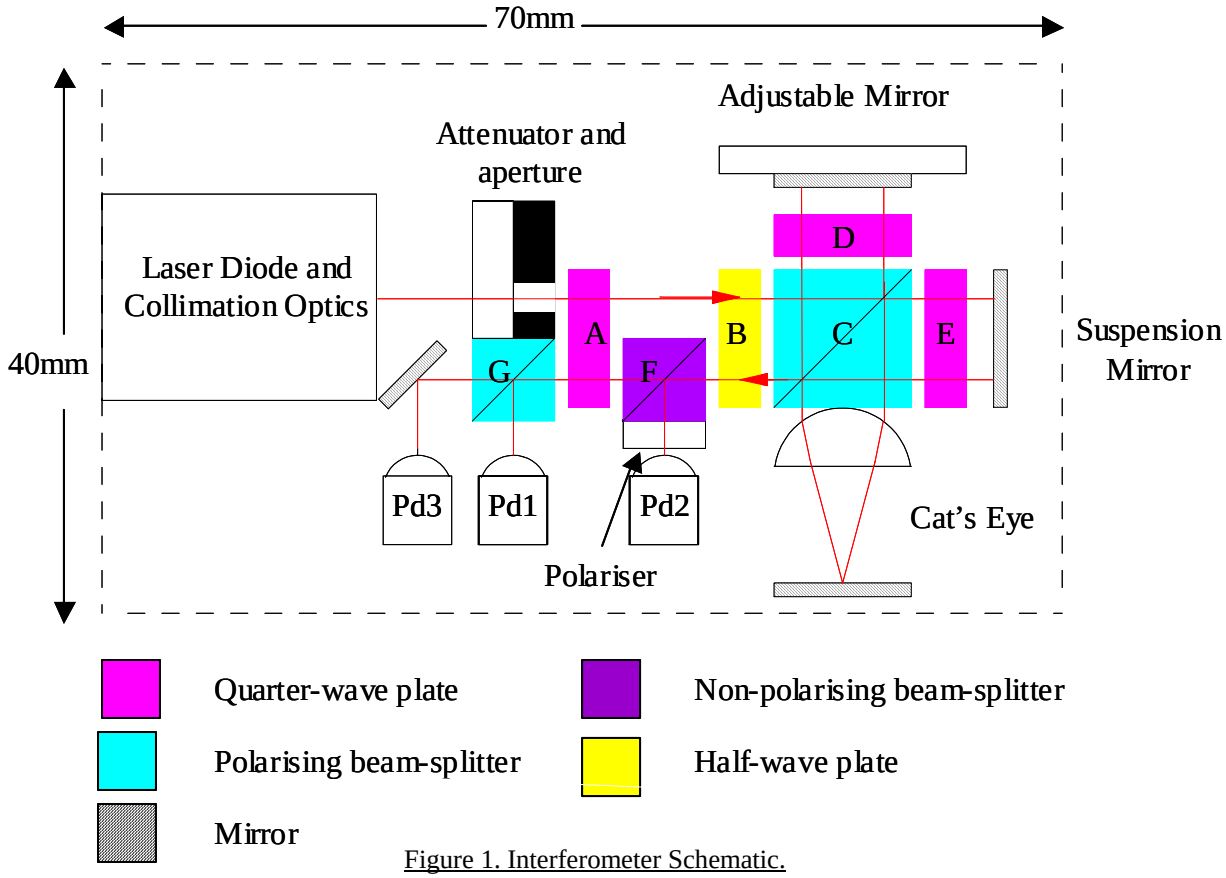

Figure 1. Interferometer Schematic.

The laser diode is orientated such that its plane of polarisation is vertical and after being attenuated its radiation becomes circularly polarised by quarter-wave plate A. The intensity after the attenuator is, I_{in}. The attenuator is necessary to ensure that optical feedback from imperfect quarter-wave plates does not destabilise the laser. The laser beam then passes through the half-wave plate B with its optic axis inclined at 22.5°. The passage of the input beam through the quarter wave plate is not necessary for the interferometer to function. We have adopted this configuration as a matter of convenience of construction although the quarter waveplate also helps to eliminate stray back reflections into the laser of polarisations that could make the laser unstable. Approximately equal intensities of two orthogonal polarisations (in-plane and perpendicular to the plane of figure 1) pass through the polarising beamsplitter C and into the measurement and reference arms of the interferometer. The quarter wave plates D and E force the beams in each arm to be first reflected from the cat's eye before exiting through the same face of the polarising beam splitter that they entered, after two reflections from their respective mirrors. The tilt of the reference mirror can be adjusted *in situ* by a simple arrangement of fine-threaded screws. A small amount of adjustment of the reference arm path length could also be achieved by this method if necessary. On exiting the beam-splitter the two polarisation components are again rotated by 45° by the half-wave plate B and pass through a non-polarising beam-splitter F. A polariser selects the horizontal polarisation component from the reflected beam and interference fringes are focused onto a photodiode, Pd2. The un-reflected beam passes through the quarter-wave plate, A, and is split into two polarisations by a polarising beam-splitter, G. Interference fringes with a phase difference of π are then focused onto two further photodiodes, Pd1 and Pd3. These two fringe outputs are shifted by $\pm\pi/2$ with respect to output Pd2. An analysis using Jones matrices shows that the output intensities, ignoring reflection losses, are then given by equation (1) with $I_{out} = \frac{I_{in}}{4}$. The displacement is calculated as $\Delta z = \frac{\Delta\phi}{2\pi} \cdot \frac{\lambda}{4}$ and the minimum sampling frequency required to track a mirror speed of 1mms^{-1} is 12.6kHz (from equations (3) and (4), but including the double-pass of the proposed interferometer). A convenient way of evaluating the difference signals in Advanced LIGO is to use the differential inputs of the ADC's. The two outputs must then be sampled sufficiently rapidly (preferably simultaneously) such that changes in the radius of the Lissajous figure do not produce significant distortion of the derived displacement.

An interferometer was constructed on an optical table with standard optical mounts to measure the key characteristics of the device. In the laboratory experiments the lens and photodiodes were not integrated as suggested in figure 1. The lenses had focal lengths of 50mm.

We used a Hitachi 6314MG laser diode operating at approximately 635nm and 30mA, corresponding to approximately 3mW optical output, which is the typical rating for the device. The diode laser was powered using a Thorlabs LD2000 laser control module that used the laser's on-chip photodiode for intensity feedback. Photocurrents from the three diodes were converted into voltages using AD711 trans-conductance amplifiers and two further OP07's were used to subtract the signals with unity gain. Radii of the Lissajous figures were of the order of 1V with feedback resistors of 220kΩ and therefore the photocurrents were about 4μA in magnitude corresponding to about 10μW of optical power. No significant change in fringe visibility was observed with the laser under these conditions. However when the diode was first used at lower power, modulation of the visibility in accordance with the discussion given in

section 3 was seen. Data analysis was performed using hardware and software supplied by Mark Zumberge and collaborators at UCSD[11] which performed a sophisticated elliptical fit to the two interference outputs, rather than the simpler algorithm, equation (2). Voltages were sampled at 50kHz and decimated to 200Hz for saving in a data file. The ADC resolution was 12-bits over a peak-peak maximum input range of 10V. The raw data file of calculated values of ϕ, equation (1), were first high pass filtered. In practice this was achieved by first low-pass filtering with a 1Hz single pole filter (Matlab FILT function) and then subtracting from the original data. Data files of 100s of filtered data were divided into sections of 10s, fast Fourier transformed and the resulting spectra averaged.

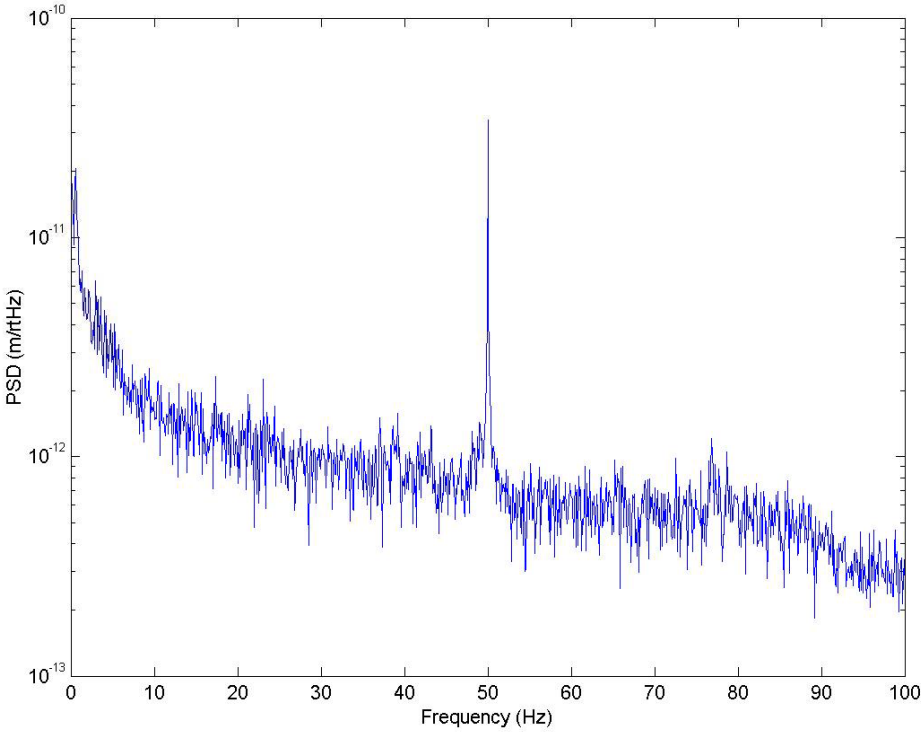

Figure 2. Displacement noise spectral density at nominal *z* = 12mm.

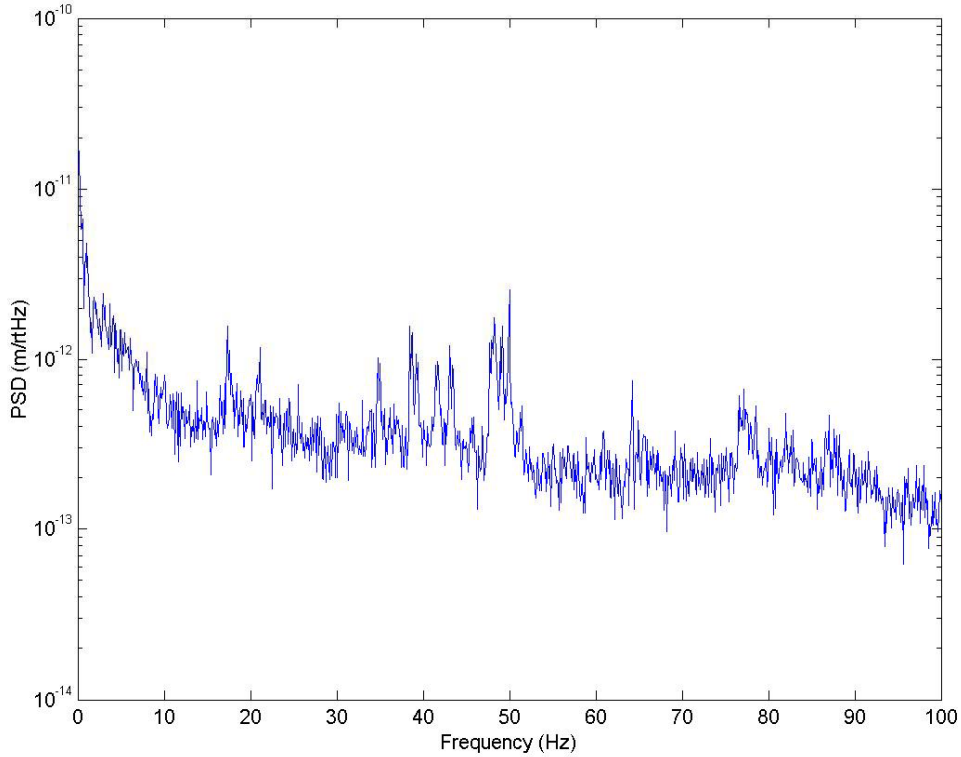

Figure 3. Displacement noise spectral density at nominal *z* = 13.5mm.

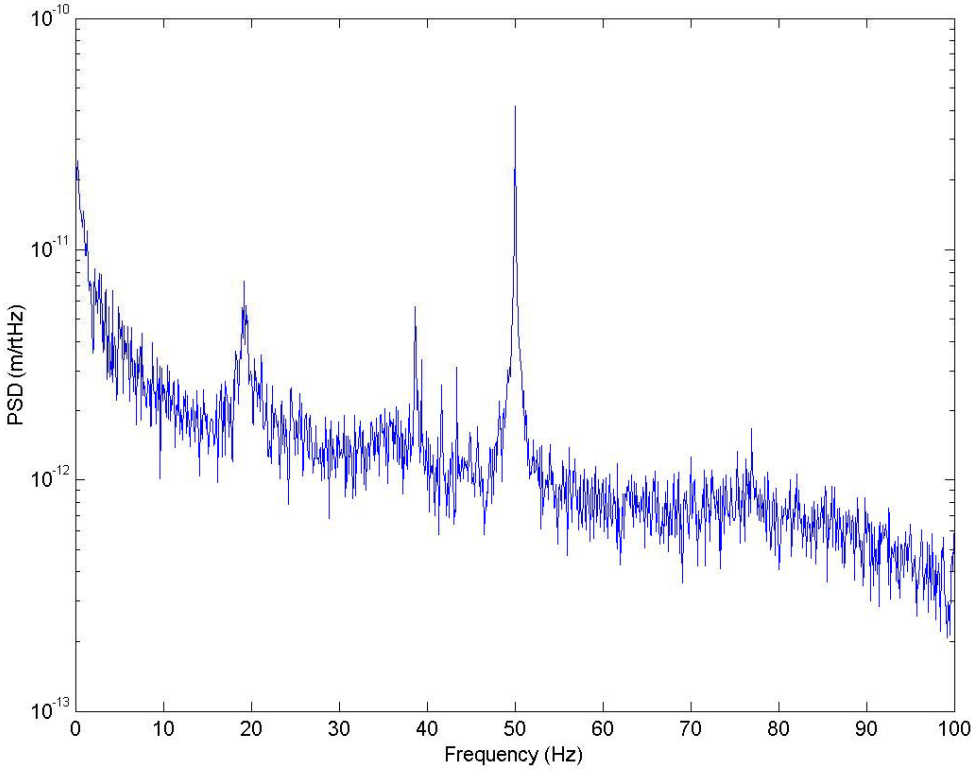

Figure 4. Displacement noise spectral density at nominal *z* = 15mm.

Tilt, θ, of the target mirror in the test set-up produced a surprisingly large change in the visibility of the fringes: visibility was reduced by a factor of 2 for $\theta \approx 5\times10^{-3} rad$. This is still being investigated. In the test configuration the distance between the target mirror and the cat's eye lens was approximately 90mm and the focal length of the cat's eye lens was 50mm.

5 Sensitivity

If there is a voltage uncertainty of δv_x and δv_y associated with each sample of the Lissajous pattern, the resulting uncertainty in the phase will be:

$$\delta\phi = \frac{2\pi}{v_0}\left(\delta v_x \cos\phi + \delta v_y \sin\phi\right) \tag{6}$$

Where v_0 is the radius of the pattern measured in volts. Assuming that the uncertainties are independent we can write:

$$<\delta\phi^2> = \left(\frac{2\pi}{v_0}\right)^2 \left(<\delta v_x{}^2>\cos^2\phi + <\delta v_y{}^2>\sin^2\phi\right) \tag{7}$$

In the case of shot noise we would expect:

$$<\delta v_x{}^2> \propto I_{out}\left(1+V\cos\phi\right) \tag{8a}$$

& $$<\delta v_y{}^2> \propto I_{out}\left(1+V\sin\phi\right) \tag{8b}$$

For the purposes of this document we will ignore the dependence of the uncertainty on the value of ϕ in our estimation of the sensitivity. We can estimate the limit to the resolution due to discretisaton noise of the ADC by assuming that variations at its input, due mainly to drift, produce a random Gaussian sampling. According to the data given in the section above, the minimum detectable voltage detectable in a sampling time of 1s is very approximately 11μV. This corresponds to a minimum displacement of about 3×10^{-13} m/rt(Hz). We can also estimate the shot noise in each difference signal to be about 3μV with correspondingly slightly smaller minimum displacement sensitivity.

Displacement data were taken at three target mirror positions that correspond to approximately equal lengths of measurement and reference arms (as judged with a steel rule and possibly a large Abbe offset!), and 1.5mm either side. In figures 2, 3 and 4 we show the noise spectra for these positions. The results are encouraging and imply that, at a target mirror position close to the point where the interferometer arms are equal in length, the device is capable of reaching

the shot noise limit. This seems at odds with the estimated discretisation noise given above and this needs to be further investigated. Excess noise below 100Hz, including the 50Hz peak, increases as the difference in arm-lengths increases. This is possibly due to intensity fluctuations changing the amplitudes of the voltages of a pair of outputs or, perhaps due to phase noise in the laser diode. Certainly there is a 'common mode' noise source that is minimised when the path lengths are equal.

6 Conclusions

We have developed a homodyne interferometer that appears to satisfy the requirements of the Advanced LIGO OSEMs. It is possible that we may be able to achieve shot noise limited performance with a higher resolution ADC (16-bits in Advanced LIGO) and, when the nature of the excess noise is understood, achieve a larger range with this resolution.

The device does not employ ac modulation and so stiff shielded cable should not be necessary. Further the leads carrying changing output photocurrents are at zero voltage. The device should be vacuum compatible.

The one outstanding issue is the reliability of the laser diode. It is difficult to obtain accurate figures from manufacturers for the MTBF. However figures between 10^4-10^5 Hrs (approximately 1-10 years) are quoted. Resolution of this problem could be achieved by using diodes at 780nm, which may be more reliable. If necessary we could include 2 laser diodes in each OSEM. This could be done using a further polarising beam splitter on the input and rotating the plane of polarisation of the second diode by 90^o with respect to the first. In figure 1 we have assumed that we house the diode laser in a Thorlabs focusing package, if we dispensed with their external barrel mount for the laser and collimator, the design could be more compact and space could be found for a second laser diode. In figure 1 we have assumed that the optical components are embedded in a slotted metal base. The design could be more compact and robust if the components could be bonded together.

7 Acknowledgements

The authors would like to express their gratitude to Gordon Rodger of National Physical Laboratory UK for useful discussions and excellent cooperation. We thank Mark Zumberge and his colleagues at UCSD for making their fringe interpolation hardware and software available for this study. We also thank the members of the ALUK team for stimulating discussions and Giles Hammond and Fabian Pena-Arellano of the Birmingham Gravitation Group for their contributions to the early phases of this development.

8 References

[1] Downs, MJ and Raine, KW Precision Engineering 1,2 85-8 (1979).

[2] Gonda, S *et al* Rev. Sci. Inst. 70, 3362-8 (1999).

[3] Raine, KW and Downs, MJ, Optica Acta 25, 549-58 (1978).

[4] Downs, MJ and Rowley, WRC, Precision Engineering 15, 281-6 (1993).

[5] LIGO-E040108-00-K, K.A. Strain *et al*, "Recommendation of a design for the OSEM sensors" (2004).

[6] Gray, MB *et al*. Optical and Quantum Electronics 31, 571-582 (1999).

[7] Inoue S, Lathi, S and Yamamoto, Y, JOSA B 14, 2761-6 (1997).

[8] Longhurst RS Geometrical and Physical Optics. 3rd edition p331 Longman (1973).

[9] NPL. web-link: http://www.npl.co.uk/length/dmet/services/equipment/interferometers.html (current 18/03/04)

[10] Greco, V, Molesini, G and Quercioli, F, Rev. Sci. Instrum, 66 3729-34 (1995).

[11] Zumberge, MA *et al* Appl. Opt, 43, 771-? (2003).